HIV-1 infection reduces NAD capping of host cell snRNA and snoRNA

Barbora Benoni,[1,2] Roberto Benoni,[1] Jana Trylcova,[1] Katarzyna Grab,[3] Jan Pačes,[4] Jan Weber,[1] David Stanek,[4] Joanna Kowalska,[3] Lucie Bednarova,[1] Zuzana Keckesova,[1] Lenka Gahurova,[1,5] and Hana Cahova[1*]

[1] Institute of Organic Chemistry and Biochemistry of the CAS, Flemingovo náměstí 2, Prague 6, Czechia
[2] Charles University, First Faculty of Medicine, Prague, Czechia
[3] Division of Biophysics, Faculty of Physics, University of Warsaw, Pasteura 5, 02-093 Warsaw, Poland
[4] Institute of Molecular Genetics of the Czech Academy of Sciences, Vídeňská 1083, Prague 4, Czechia,
[5] Department of Molecular Biology and Genetics, Faculty of Science, University of South Bohemia, Branišovská 1760, 37005 České Budějovice, Czechia
* To whom correspondence should be address. Tel: +420 220 183 124, Email: cahova@uochb.cas.cz

Abstract

NAD is a key component of cellular metabolism and also serves as an alternative 5'cap on short noncoding RNAs. The function of NAD in RNA, however, remains poorly understood. We investigated NAD capping of RNAs in HIV-1 infected cells, as HIV-1 is responsible for the depletion of the NAD/NADH cellular pool and causes intracellular pellagra. We used NAD captureSeq on HIV-1 infected/noninfected cells and revealed that four snRNAs (U1, U4ATAC, U5E, and U7) and four snoRNAs (SNORD3G, SNORD102, SNORA50A, and SNORD3B) lost their NAD cap when infected with HIV-1. Here, we provide evidence that the loss of the NAD cap increases the stability of the U1-HIV-1 pre-mRNA duplex. We also show that decreasing the amount of NAD-capped U1 snRNA by overexpressing the NAD RNA decapping enzyme DXO leads to a marked increase in HIV-1 infectivity. Moreover, an experimental increase of NAD capped RNAs improves the efficiency of splicing of HIV-1 and cellular RNAs and lowers HIV-1 infectivity. Our experiments show a dual role of U1 snRNA in HIV-1 infection and present the first clear role of NAD-capped RNAs in eukaryotic antiviral responses with a potential overlap into cellular splicing.

Introduction

To date, more than 170 RNA modifications have been discovered.(1) Among the least explored RNA modifications are 5' noncanonical RNA caps, including CoA,(2) NAD,(3) and dinucleoside polyphosphate RNA,(4) the last of which was recently discovered in bacteria. Because they are typically detected through LC-MS analysis of digested RNA, there is no information on RNA sequences bearing these caps. Only NAD captureSeq(5, 6) allows identification of NAD-RNA sequences in various cellular organisms (e.g. *S. Aureus*,(7) *S. Cerevisia*,(8) human cells,(9) and plants(10)). Furthermore, NAD has been detected as a 5' RNA cap attached to small regulatory RNA in bacteria(5) and various mRNAs in higher organisms, yet the role of this cap remains unclear.

Because HIV-1 infection of human cells depletes the cellular pool of free NAD,(11) we envisaged it as a physiologically important model system in which to study the role of the NAD RNA cap(11). There are two alternative mechanisms responsible for NAD depletion: first, there is increased activity of CD38 in HIV-1 infected cells, which reduces the NAD pool;(12-14) the second mechanism includes activation of poly (ADP-ribose) polymerases (PARPs) induced by oxidative stress during HIV-1 infection.(15, 16) The PARPs consume NAD and thus trigger de novo niacin synthesis, which starts with tryptophan oxidation. The depletion of tryptophan leads to further immunosuppression.(17) Moreover, it has been reported that

nicotinamide acts as an inhibitor of HIV-1 infection.(18) For this reason, niacin was suggested as a potential AIDS preventive factor.(19, 20)

In light of the recent discovery of NAD as a cap on different RNA types,(9) we explore the influence of HIV-1 infection on NAD RNA capping. Here, we report that subsets of cellular snRNA and snoRNA lose the NAD cap after HIV-1 infection. Among the identified RNAs that lose the NAD cap upon HIV-1 infection, we detected U1 snRNA, which is essential for viral replication.(21, 22) We found that in comparison with 7,7,2-trimethylguanosine (TMG) capped U1 snRNA,(23) the NAD cap has a destabilizing effect on U1 snRNA binding to viral pre-mRNA. This indicates that the NAD RNA cap reduces U1 snRNA binding with the viral RNA target and might protect cells from HIV-1 infection. To test this hypothesis, we overexpressed and knocked down the NAD decapping enzyme DXO and monitored HIV-1 production. The overexpression of DXO, which decreases cellular levels of NAD capped RNAs, results in higher virus infectivity. To study whether repletion of NAD influences HIV-1 infection, we supplemented cells with Nicotinamide (NAm, direct NAD precursor) and we measured changes in U1 NAD capping and infectivity of HIV-1. We observed general effect of NAD capping on cellular and viral mRNA splicing. This finding may indicate that NAD RNA caps play a role in hindering HIV-1 replication. Here, we propose mechanism how NAD capping of U1 may influence HIV-1 viral production.

Material and Methods

Cell culture.
The human CD4+ T-cell line MT-4 (NIH AIDS Reagent Program, Division of AIDS, NIAID, NIH from Dr. Douglas Richman) and the human embryonic kidney HEK293T cell line (American Type Culture Collection, LGC Standards, UK) were cultured under standard conditions at 37 °C under a humidified (>90%) atmosphere of 5% CO2/95% air. The MT-4 cell line was cultured in RPMI 1640 with L-Glutamine and 25 mM Hepes supplemented with 10% FBS, penicillin (100 U/mL) and streptomycin (100 µg/mL) (all Sigma-Aldrich). The HEK293T cell line was cultured in DMEM high glucose supplemented with 10% FBS, penicillin (100 U/mL) and streptomycin (100 µg/mL) (all Sigma-Aldrich).

HIV-1 culture.
MT-4 cells were infected with a cell-free HIV-1 strain NL4-3, which was generated by transient transfection of HEK293T cells with a pNL4-3 plasmid (obtained through NIH AIDS Reagent Program, Division of AIDS, NIAID, NIH from Dr. Malcolm Martin). The infected cultures were subsequently expanded by co-cultivation: 48 h post-infection, cell culture supernatants containing viral particles and infected cells were added to uninfected MT-4 cells ($5*10^5$ cells per mL) at a ratio of 1:9. The co-culture was synchronized by three successive additions of infected culture supernatant to uninfected MT-4 cells ($5*10^5$ cells per mL, the ratio of 1:9, 27 h interval). For the NAD repletion, the medium was supplemented with 10 mM of nicotinamide (NAm, Sigma-Aldrich), the NAD precursor (11, 18).The cell cultures were incubated for additional 40 hours and then harvested.MT-4 cells infected and noninfected were collected by centrifugation (225× g, 5 min, at 20 °C). Cells pellets were washed with PBS and cells were lysed with RNAzol reagent (Sigma-Aldrich). Virus-containing supernatants were filtered (0.45 µm pore size cellulose-acetate filter (VWR)), and stored at −80 °C.HIV-1 titer was measured by 10-fold serial infection of TZM-bl cells (NIH AIDS Reagent Program, Division of AIDS, NIAID, NIH from Dr. John C. Kappes and Dr. Xiaoyun Wu) in triplicate, calculated by Reed-Muench method and expressed as 50% tissue culture infectious dose.

NAD/NADH measurement.
NAD total levels in MT-4 cells and MT-4 cells infected by HIV-1 were assessed using the NAD/NADH Quantification Kit (Sigma-Aldrich) according to the manufacturer's protocol. $2*10^5$ MT-4 cells from each

set were pelleted and the extract together with NADH standards (all in duplicates) were measured in a 96 well flat-bottom plate in three replicates. To evaluate the efficiency of NAD repletion, eight differently prepared MT-4 cell lines (MT-4, MT-4 infected by HIV-1, MT-4 with DXO OE, MT-4 with DXO OE and infected by HIV-1, all conditions with or without NAD repletion) were measured as described and expressed as fold-increase of NAD levels.

Isolation of small RNA fractions from the cell culture.
Small RNA fraction was purified according to the RNAzol manufacturer's protocol. The RNA concentration was determined on NanoDrop ONE (ThermoFisher Scientific) and the RNA sample quality control was performed on a 4200 TapeStation System (Agilent).

LC-MS method for MRM analysis.
sRNA from each sample was incubated in 50 mM sodium acetate buffer (pH 4.5, Sigma-Aldrich) with 10 U of NucleaseP1 (NuP1, Sigma-Aldrich) or mock treated with water (negative control) for 1 hour at 37 °C. The samples were filtered with Microcon-10 kDa columns (Merck) and the filter was washed once with 100 µL of water. The wash and the filtrate were combined, dried using SpeedVac, and resuspended in 10 µL of water with 0.1% formic acid and 2% acetonitrile (Sigma-Aldrich). For each sample, 8 µL of the dissolved material was injected. The quantification of NAD+ was performed using SCIEX QTRAP 6500+ instrument with a Kinetex C18 column (1.7 µm, 2.1 mm × 100 mm, Phenomenex). Mobile phase A was water with 0.1% formic acid, and mobile phase B was 100% acetonitrile with 0.1% formic acid. After optimization 3 transitions were selected and used to create an MRM method. For the LC, method with a constant flow rate 0.3 mL/min was developed and the gradient composition was as following: 2% B for 0.5 min; linear increase till 9 min to 50% B; another linear increase to 98% in 1 min, and maintain at 98% B for 5 min before returning linearly to 2% B over 0.1 min. The oven temperature was 60 °C. ESI source was used with curtain gas of 40 (arbitrary units) and ion spray voltage of 5.5 kV. The ion source gases were 40 and 50 (arbitrary units), and the drying gas temperature was 400 °C. The entrance potential was +13 V. The detector was operated in positive ion mode. For the MRM method, the first precursor ion was [M + H]+ at *m/z* 664.15 and the three different transitions [M + H]+ at m/z 428 (DP: +113 V, CE: +37 V, CXP: 10), [M + H]+ at m/z 523.9 (DP: +106 V, CE: +24 V, CXP: 28) and [M + H]+ at m/z 542.0 (DP: +107 V, CE: +20 V, CXP: 16).

Quantification of NAD-cap RNA.
A total of 2000 µg of lRNA from MT4 cells was divided into four aliquots. After digestion with NuP1, each aliquot was spiked with increasing concentration of NAD (Sigma-Aldrich). After MRM analysis of all the aliquots the area under the peak was calculated and plotted against the concentration of the spiked NAD. The experimental points were fitted with a liner regression and the intercept with X-axis represent the concentration of the NAD-cap in the sample. The quantification was repeated three times and the final value was obtained from the average of the three measurements with relative SD.

U1 RNA capture and quantification.
Annealing of 5 nmol of biotinylated U1 probe (Table SI1) to 50 µg of sRNA was performed in a buffer supplemented with 10 mM Tris, 50 mM NaCl and 1 mM EDTA, pH 7.8, by a temperature slowly decreasing from 65 °C to 25 °C. Dynabeads™ MyOne™ Streptavidin C1 (ThermoFisher Scientific) were prepared based on manufacturer protocol. Briefly, the beads were resuspended and 100 µL was transferred to a new tube and washed 3 times with 1x binding and washing buffer (5 mM Tris-HCl, 0.5 mM EDTA, 1M NaCl, pH 7.5).

Since the beads are not supplied in RNase-free solutions, they had to be washed twice in solution A (DEPC-treated 0.1 M NaOH and 0.05 M NaCl) and twice in solution B (DEPC-treated 0.1 M NaCl). After washing, the beads were resuspended in twice original volume of 2x binding and washing buffer and an equal volume of biotinylated U1 probe annealed to RNA was added. Samples were incubated for 15 mins at room temperature using gentle rotation. The beads were washed twice with 1x binding and washing buffer and resuspended in RNase-free water. To dissociate the captured U1 RNA, samples were incubated for 10 minutes at 75°C. The concentration of released U1 RNA was measured on QUBIT and the purity of samples was validated via 12.5 % PAGE. The rest was digested by NuP1 for 1 hour at 37 °C as described previously. Samples were washed, dried using SpeedVac and dissolved in 10 µL water with 0.1% formic acid and 2% acetonitrile. 8 µL of the samples were injected into SCIEX QTRAP 6500+ instrument and measured as described previously. Standards were prepared with increasing concentrations of NAD (Sigma-Aldrich). After MRM analysis of all the aliquots, the area under the peak was calculated and plotted against the concentration of the NAD. The experimental points were fitted with linear regression and the intercept with X-axis represent the concentration of the NAD-cap in the sample. The amount of NAD cap was normalized to the concentration of the injected sample in fmol and expressed as the percentage of U1 RNA capped with NAD. The quantification was repeated three times and the final value was obtained from the average of the three measurements with relative SD.

NAD captureSeq library preparation.

NAD captureSeq libraries from four biological replicates for each sample were performed as described(6). Briefly, only short fraction of RNA from MT-4 cells infected by HIV-1 and MT-4 cells noninfected were used for the library preparation. The most critical step is the enzyme reaction catalyzed by ADP-ribosylcyclase (ADPRC, Sigma-Aldrich), which is an enzyme specific only for NAD-capped RNA but inactive on canonical RNA. Samples not treated by ADPRC were used as a negative control for non-specifically bound RNA. 100 µg of sRNA for each sample was incubated with 4-pentyn-1-ol (10%, Sigma-Aldrich) and ADPRC (2.5 µg) in 50 mM Na-HEPES (pH 7.0, Sigma-Aldrich) and 5 mM $MgCl_2$ (Sigma-Aldrich) for 30 min at 37 °C. The reaction was stopped by phenol/ether (Roti-Aqua-Phenol: Carl Roth, Diethyl ether: Penta) extraction and RNA was ethanol precipitated. NAD-capped RNA was then biotinylated (biotin-PEG3-azide, 250 mM, Jena Bioscience) via a copper-catalyzed azide-alkyne cycloaddition (CuAAC) in a freshly prepared mixture of CuSO4 (1 mM, Sigma-Aldrich), THPTA (0.5 mM, Sigma-Aldrich) and sodium ascorbate (2 mM, Sigma-Aldrich) for 30 min at 25 °C, with shaking at 350 r.p.m. The biotinylated RNA was purified by phenol/ether extraction and ethanol precipitated. Mobicol Classic columns (MoBiTec, GmbH) were assembled and 50 µl of streptavidin Sepharose (GE Healthcare) was transferred to each column. After washing the beads by adding three times 200 µL of immobilization buffer (10 mM Na-HEPES, 1 M NaCl and 5 mM EDTA, pH 7.2) to each column and centrifuge at ≥16,100 g for 1 min at rt, the beads were blocked with acetylated BSA (100 µg/ml, Sigma-Aldrich) in 100 µL of immobilization buffer for 20 min at 20 °C, with shaking at 1,000 r.p.m. After three more washes, the RNA was immobilized on the beads for 1 h at 20 °C, with shaking at 1,000 r.p.m. The beads were washed five times with 200 µL of streptavidin wash buffer (50 mM Tris-HCl and 8 M urea, pH 7.4, both Sigma-Aldrich), then equilibrated by washing three times with 200 µL of 1x standard ligation buffer (50 mM Tris-HCl, 10 mM $MgCl_2$, pH 7.4), blocked with acetylated BSA, and washed three more times with 1x standard ligation buffer as described previously. 30 µL of ligation mixture containing adenylated RNA 3'adaptor (5 µM), 1x standard ligation buffer, DMSO (15%, Sigma-Aldrich), acetylated BSA (1.5 µg), 2-mercaptoethanol (50 mM, Sigma-Aldrich), T4 RNA ligase (15 U, Thermo Fisher Scientific), and T4 RNA ligase 2, truncated K227Q (300 U, New England BioLabs) was added to the beads

and the mixture was incubate at 4 °C overnight (≥16 h). The biotinylated RNA was rebound by adding 7.5 µL 5 M NaCl and incubated for 1 hour at 20 °C, with shaking at 1,000 r.p.m. After washing the beads five times with the streptavidin wash buffer, they were equilibrated by washing three times with 1× first-strand buffer (50 mM Tris-HCl, 75 mM KCl and 5 mM $MgCl_2$, pH 8.3), blocked with acetylated BSA, and washed another three times with 1× first-strand buffer. The beads were covered with 30 µL of reverse transcription mixture containing dNTPs (0.5 mM each, New England BioLabs), acetylated BSA (1,5 µg), DTT (5 mM), 1x first strand buffer, reverse primer (5 µM), and Superscript III reverse transcriptase (300 U, Thermo Fisher Scientific) and incubated for 1 hour at 37 °C. The rebinding procedure was repeated and samples were washed five times with streptavidin wash buffer and three times with 1x ExoI buffer (Thermo Fisher Scientific). The beads were blocked with acetylated BSA in ExoI buffer and again washed three times with 1x ExoI buffer. The free primers were digested by adding 30 µL of 1x ExoI buffer and 30 U of ExoI (Thermo Fisher Scientific) and the mixture was incubated for 30 min at 37 °C. The beads were washed five times with streptavidin wash buffer and three times with immobilization buffer. The RNA was digested by adding 100 µl of 0.15 M NaOH solution and incubating for 25 min at 55 °C. The columns were centrifuged and washed with 100 µl of H_2O. The flow-through was ethanol precipitated and the cDNA pellet was dissolved in 19 µl of Terminal deoxynucleotidyl transferase (TdT) tailing mixture containing 1x TdT buffer (Thermo Fisher Scientific) and CTP (1.25 mM). After adding 20 U of TdT (Thermo Fisher Scientific), the mixture was incubated in thermocycler for 30 min at 37 °C and after the enzyme was thermally denatured by heating to 70 °C for 10 min. Then, the second adaptor was ligated on the cDNA by adding 60 µl of reaction mixture containing 1x standard ligation buffer, cDNA anchor (5 µM each strand), ATP (10 µM), and T4 DNA ligase (120 Weiss U, Thermo Fisher Scientific) and incubating for 16 h at 4 °C. PCR amplification was performed with barcoded reverse PCR primers in 25 cycles in Taq DNA Pol reaction buffer 1 × (Thermo Fisher Scientific), with 1 µM of each reverse barcoded primer and forward primer (Table SI1), 0.2 mM dNTPs (each) and 2.5 U of DreamTaq DNA Polymerase (Thermo Fisher Scientific) in 50 µL of total reaction mixture. Initial denaturation was performed at 95 °C for 3 min, following by annealing for 30 s at 68 °C, elongation for 30 s at 72 °C and denaturation for 30 s at 95 °C. Final extension was performed at 72 °C for 5 min. PCR reaction mixture was loaded on 2.5% agarose gel (140 V for 2 h) and post-stained with SYBR gold (Thermo Fisher Scientific). Fractions between 100–400 nt were cut and DNA was extracted from the gel by Monarch DNA Gel extraction Kit (NEB). Multiplexed samples were submitted to the IMG Genomics and Bioinformatics facility for library synthesis using the NextSeq® 500/550 High Output Kit v2, 75 cycles (Illumina) and sequencing on a NextSeq 500/550, Illumina.

Small RNA-seq library preparation.

To verify the amounts of sRNAs in samples, three biological replicates of sRNA from MT-4 cells and MT-4 cells infected by HIV-1 were submitted for miRNA (LP-170) library preparation to SEQme. The library synthesis was done using the NEBNext®Small RNA Library Prep Set for Illumina with NEBNext Multiplex Oligos for Illumina (Index Primers Set 1-3) and sequenced on a NovaSeq 6000 System (SE 50 bp, 350-400 milions of reads, DS-270).

Long RNA-seq library preparation.

To evaluate the splicing changes in MT-4 cells under various conditions, three biological replicates of lRNA from MT-4 cells, MT-4 cells infected by HIV-1 and MT-4 cells with DXO OE, all mentioned conditions with or without NAD repletion were submitted for library preparation to the IMG Genomics and Bioinformatics facility. KAPA RNA HyperPrep Kit with RiboErase was used to prepare the libraries and the sequencing was

performed using the NextSeq® 500/550 High Output Kit v2, 75 cycles (Illumina) and on a NextSeq 500/550, Illumina.

Data processing and bioinformatic analysis.
Adapters and low-quality bases were trimmed using TrimGalore! v.0.4.1. Because of a bias at the ends of the reads, additional 5 bases were trimmed from both 5' and 3' end of the reads. Reads were mapped to the human GRCh38 genome and HIV-1 HIVNL43 NC_001802.1 genome using Hisat2 v.2.0.1. To analyse NAD presence at HIV RNA cap, we quantified RPM in the first 200 bp of HIV transcribed region and quantified the enrichment of ADPC-treated samples over controls using Seqmonk v1.47.2. Enrichment of human shortRNAs was quantified as RPM in ADPRC-treated over control samples using Seqmonk v1.47.2. To select the best candidate shortRNAs with depletion or increase of NAD-cap abundance after HIV infection, we applied a set of criteria removing shortRNAs with low read count and/or low enrichment over control (-ADPRC): (I) raw read count has to be 2 or higher for at least 2 replicates of at least one sample type (+/-ADPRC +/- HIV infection), (II) enrichment over control higher than 2 in at least one replicate and enrichment above 1 in at least one additional replicate in either HIV infected or non-infected samples, (III) of all 4 replicates, 2 or more have to show depletion/increase in the same direction (difference between HIV non-infected and infected above 0.2), and neither in the opposite direction, and maximum 2 replicates the lack of enrichment (enrichment <1), (IV) total raw read count in combined replicates of +ADPRC samples (either non-infected or infected) above 20, (V) the number of reads in +ADPRC samples above 5 in the replicates showing enrichment above 1. Differential expression of sRNAs of all sRNA classes annotated within Seqmonk v1.47.2 (GRCh38v100 genome annotation) was analysed using DESeq2 implemented within Seqmonk v1.47.2. Splicing efficiency of HIV-1 transcript was analysed as ratio of read count in random regions within introns to read count in size matched random regions in exon 3. Sequences of main donor and acceptor splice sites in HIV-1 main splicing variants (according to (24)) were obtained from (25) and matched against HIV-1 HIVNL43 NC_001802.1 genome to generate genomic coordinates of exons and introns. Splicing efficiency of cellular transcripts was quantified as ratio of reads in introns to reads in exons for 1000 genes with the highest expression in combined replicates of untreated MT-4 cells quantified using RNA-seq quantitation pipeline within Seqmonk v1.47.2.

Deep sequencing data validation through RT-PCR.
Real-time PCR was performed to verify the NAD captureSeq data. Three biological replicates of sRNA from infected and noninfected MT-4 cells and cDNA samples after NAD captureSeq were measured in two technical repeats on LightCycler 480 II (Roche) by Luna Universal One-Step RT-qPCR Kit (New England BioLabs) according to the manufacturer protocol. Briefly, 20 µl reaction mix consisting of buffer, enzyme mix, forward and reverse primer (0.4 µM, Table SI1) and 50-100 ng template was prepared. PCR was conducted with the following program: reverse transcription 55 °C for 10 min, initial denaturation at 95 °C for 60 s, followed by 40 cycles of 95 °C for 10 s and 53 °C for 30 s. Finally, a melting curve was performed from 37 °C to 95 °C. The Cp values were calculated by LightCycler 480 Software and the reciprocal values were plotted.

Chemical synthesis of TMG cap (TMGpppApG).
To enable synthesis of highly homogenous 5'-TMG-capped RNA by in vtro transcription we designed a trinucleotide TMG cap analog (TMGpppApG or $m_3^{2,2,7}$GpppApG) following the synthetic pathway described previously for NAD-derived trinucleotides.(26) Briefly, pApG dinucleotide was synthesized by

automated solid-phase synthesis, imidazole-activated, and coupled with 2,2,7-trimethylguanosine diphosphate ($m_3^{2,2,7}GDP$) in DMSO in the presence of anhydrous magnesium chloride ($MgCl_2$). The final compound was purified by ion-exchange chromatography (DEAE Sephadex A-25) using a linear gradient of triethylammonium bicarbonate buffer, followed by semi-preparative reversed phase HPLC. The final product of the reaction was lyophilised three times and its structure was confirmed by high-resolution MS (for structure of TMGpppApG and detailed synthetic procedure, see Supporting Information).

RNA in vitro transcription.

In vitro transcription was performed as described (27) in a 50 µL mixture (0.2 µM of template DNA (Table SI1), 1 mM of each NTP (New England BioLabs), 5% dimethyl sulfoxide (DMSO, New England BioLabs), 0.12% triton X-100 (Sigma-Aldrich), 10 mM dithiothreitol (DTT), 4.8 mM $MgCl_2$ (Sigma-Aldrich), 1× reaction buffer for T7 RNAP (New England BioLabs) and 125 U of T7 RNAP (New England BioLabs). For capped RNA, 8 mM of NAD (Sigma-Aldrich) or TMG cap was added. For the production of 20 nt long U1 RNA containing pseudouridine, the UTP was replaced with pseudo-UTP (Jena Bioscience). The mixture was incubated for 2 h at 37 °C. For higher yield, T7 RNAP was added again into the mixture and incubated for additional two hours. The DNA template was digested by DNAse I (New England BioLabs) at 37 °C for 45 min and the enzyme was heat inactivated at 75 °C for 10 min. To obtain only capped RNA, the samples were treated with 5′-polyphosphatase (Epicenter) for 30 min at 37 °C and then with Terminator™ 5′-phosphate-dependent exonuclease (Epicenter) for 1 h at 30 °C. Between each step, samples were purified using Clean and concentrator (Zymo).

Assessment of melting temperature by circular dichroism.

The ECD spectra were measured on a Jasco 815 spectropolarimeter (Tokyo, Japan) equipped with the Peltier type temperature control system PTC-423S/L at room temperature in spectral range from 200 nm to 350 nm, using a 0.2 cm path length with standard instrument sensitivity, with the scanning speed of 10nm/min, response time of 8 s, and 2 spectra accumulations. For measurements 26000 ng of RNA duplex with TMG-U1 RNA and/or RNA duplex with NAD-U1 was dissolved in annealing buffer (10 mM Tris, 50 mM NaCl, 1 mM EDTA pH 7,8). The final spectra were expressed as differential absorption ΔA. Melting temperature was obtained as results of measurement of CD signal at 264 nm in temperature range from 5 °C to 95 °C with temperature slope 24 °C/h, step 1 °C and time constatnt 8 sec. Each measurement was repeated 3 times. Melting temperature was calculated using sigmoid fitting by program Sigmaplot 12.5 (Systat software).

U1 RNA and HIV-1 mRNA complex stability assay.

20 nt long U1 RNA (capped either with TMG or NAD cap) and HIV-1 mRNA (Table SI1) were prepared by in vitro transcription. 150 ng of U1 RNA (TMG or NAD cap) and 150 ng of HIV-1 mRNA were mixed with ResoLight dye (1x, Roche) and annealing buffer (10 mM Tris, 50 mM NaCl, 1 mM EDTA pH 7,8). Three technical replicates were prepared three times and measured on LightCycler 480 II (Roche). High-resolution melting curves were obtained by measuring the complex stability by temperature increase to 80 °C and then decrease to 20 °C with a ramp rate 0.01 °C/s in three cycles and thus obtaining a total of 27 melting curves per sample. HRM curve analysis was performed using the LightCycler 480 Software.

Radioactively labelled U1 RNA preparation.

DNA template for U1 RNA (164 nt full length) was prepared from plasmid (U1-SP65 plasmid containing the main U1 variant RNA-U1-1) via PCR in 50 µL reaction mix consisting of DreamTaq buffer (1x, Thermo Fisher Scientific), DreamTaq DNA polymerase (1.25 U, Thermo Fisher Scientific), forward and reverse

primer (0.5 µM, Table SI1), dNTPS (2mM each, New England BioLabs) and 400 ng template. PCR was conducted with the following program: initial denaturation at 95 °C for 2 min, followed by 30 cycles of 95 °C for 30 s, 60 °C for 30 s and 72 °C 1 min, the final extension was performed at 72 °C for 5 min. PCR reaction mixture was loaded on 1% agarose gel (140 V for 2 h) and post-stained with SYBR gold (Thermo Fisher Scientific). The product bend was cut and DNA was extracted from the gel by Monarch DNA Gel extraction Kit (NEB). ^{32}P-GTP labelled U1 RNA was prepared by in vitro transcription as described previously with addition of 0.5 µL of α-^{32}P-GTP (3.3 µM, 10 µCi/µL; Hartmann analytic), with either TMG or NAD cap.

U1 RNA decapping by DXO.

150 ng of ^{32}P-GTP labelled U1 RNA was incubated with different concentrations of DXO decapping enzyme(9) (0 nM, 5 nM, 10 nM, 25 nM, 50 nM) in decapping buffer (10 mM Tris pH 7.5, 100 mM KCl, 2 mM DTT, 2 mM $MgCl_2$ and 2 mM $MnCl_2$) at 37 °C for 15 min. Reactions were stopped by the addition of RNA loading dye (Thermo Fisher Scientific) and loaded into the gel wells. Denaturing polyacrylamide gel (12.5%) was prepared from Rotiphorese gel (Carl Roth) in 1x TBE buffer and supplemented with acryloylaminophenylboronic acid (APB, 0.4%)(28). The polymerized gel was pre-run at 600 V for 30 min in 1x TBE buffer and then run at 600 V for 5 hours. The gel was incubated with phosphor imaging plate (GE healthcare), scanned using Typhoon FLA 9500 (GE Healthcare) and analysed using ImageJ.

Lentiviral vectors.

The lentiviral vectors were generated using HEK293T cells by a transient three-plasmid transfection as previously described. Briefly, the cells were transfected with 1 µg of the pMDG envelope plasmid, 1 µg of the pR8.2 packaging plasmid, and 1.5 µg of the lentiviral vector (shRNA knockdown DXO vector VB900039-9959kyv or DXO gene expression vector VB900001-2728fsj, VectorBuilder) in the mixture of Opti-MEM (200 µL, Thermo Fisher Scientific) and X-tremeGENE™ HP DNA Transfection Reagent (18 µL, Roche). Vector particles were collected from medium 48 h and 72 h posttransfection.(29)MT4 cells ($5*10^6$ cells) were infected with 1 mL of collected media, incubated for 1 hour and transferred into flasks with 5 mL of RPMI media. After 24 hours, the cells were centrifuged (225× g, 5 min, at 20 °C), washed with PBS and resuspended in 10 mL of RPMI with 10 µL of puromycin (2mg/mL, Thermo Fisher Scientific) as selection marker.

Western blot.

MT-4 cells with and without lentiviral plasmids were collected by centrifugation (225× g, 5 min, at 20 °C) and proteins were extracted using lysis buffer (RIPA Thermo Scientific, cOmplete™, EDTA-free Protease Inhibitor Cocktail, Sigma Aldrich). The protein concentration was measured on Tecan (Schoeller) and approximately 20 µg of protein lysate was loaded on the 10-well protein gels (Mini-PROTEAN TGX, Bio-Rad) and run at 120 V. Gels were wet transferred on PVDF membranes (Thermo Fisher Scientific) at 30 V for 2 hours. Primary antibody DOM3Z Rabbit PolyAb (Proteintech Europe) was diluted 1:500 and incubated overnight at 4 °C. Washes were performed with PBS 0.1% Tween-20 (PBST) before the addition of secondary antibody (1:10000, peroxidase conjugate affini pure Goat Anti rabbit IgG, Jackson Immuno research) for 1 hour at r.t. Blots were developed using enhanced chemiluminescent (ECL, Dura or Femto, Thermo Scientific) and imaged on the Azure Biosystems (model c600).

HIV-1 infectivity determination in DXO-transduced cells.

The HIV-1 infectivity and NAD repletion in DXO-transduced cells was determined by measuring HIV-1-induced cytopathic effect by XTT cell proliferation assay. Briefly, wild type MT-4 and DXO-transduced MT-4 cells were seeded at $3x10^4$ cells per well in a 96-well plate in RPMI medium (phenol red-free RPMI,

supplemented with 10% FBS, penicillin (100 U/mL), streptomycin (100 µg/mL), 2 mM L-glutamine and 4 mM HEPES, all Sigma Aldrich) with and without 10 mM NAm, infected in triplicate by two-fold serially diluted HIV-1 and cultured at 37 °C and 5% CO_2. After 4 days, 50:1 mixture of XTT salt and PMS electron-coupling reagent (both VWR) was added to the wells and incubated for 4 h at 37 °C in 5% CO_2. Formation of orange formazan dye was measured in EnVision plate reader (Perkin Elmer) at 560 nm. HIV-1 titer was calculated by Reed-Muench method and expressed as 50% tissue culture infectious dose.

Results

NAD/NADH levels in HIV-1 infected cells

It has been reported that HIV-1 infection causes intracellular pellagra, i.e. depletion of the NAD/NADH pool in the cell;(11) therefore, we measured the total concentration of NAD in control (noninfected MT4) cells and MT4 cells infected with HIV-1 (Figure 1A). Indeed, we observed an intracellular concentration of NAD in noninfected cells that was nearly four times greater than in infected ones. Since NAD is incorporated into RNA cotranscriptionally by RNA polymerase as a noncanonical initiating nucleotide(30), we hypothesized that the change in the intracellular level of NAD may also influence NAD capping of RNA. The NAD cap has been recently detected on mRNA as well as on short regulatory RNA in human cells(9). The effect of the NAD cap on mRNA has not been fully revealed, but in vitro experiments have shown that NAD-mRNA is not translated.(31) In this study, we examined the potential effect of the NAD RNA cap on short noncoding regulatory RNAs (sRNA).

We investigated the impact of HIV-1 infection on the NAD RNA cap level in an sRNA fraction and compared the absolute NAD RNA cap level in this fraction from healthy and infected cells by LC-MS. As we observed a significant decrease in the free NAD concentration in the HIV-1 infected cells, we also detected an eighteenfold decrease in the NAD cap level in the sRNA fraction from MT4 infected cells as compared with healthy cells (Figure 1B, Figure SI1). We did not observe any NAD RNA cap in HIV-1 virions (Figure SI2). This finding demonstrates that HIV-1 infection strongly influences not only the free NAD cellular concentration but also the concentration of NAD covalently attached to RNA.

NAD captureSeq of HIV-1 infected/noninfected cells

To identify RNAs with reduced NAD capping, we prepared four NAD captureSeq libraries from the sRNA fraction of MT4 noninfected and HIV-1 infected cells. The NAD captureSeq(5, 6) relies on selective reaction of ADP-ribosyl cyclase (ADPRC) with 4-pentyn-1-ol and with NAD-RNA (Figure 1C, Table SI1). After CuAAC reaction, the NAD-capped RNA is tagged with biotin and captured on streptavidin beads. The captured RNA is then reversely transcribed, and cDNA is used for preparation of the NAD captureSeq libraries. To sort out nonspecifically interacting RNA, ADPRC is omitted in negative control samples.

The sequenced NAD captureSeq libraries were mapped to both human and HIV-1 genomes (Figure SI 3A). We did not detect NAD cap on viral encoded short 5' fragments (Figure SI 3B). We detected NAD cap in 109 cellular sRNAs (2 miRNAs, 20 miscRNAs, 62 tRNAs, 12 snoRNAs, 12 snRNAs). Of these, 54 are changing between the conditions (+/- HIV). Data analysis revealed a significant loss of the NAD cap on selected sRNAs from HIV-1 infected MT4 cells. The loss of the NAD cap was most evident in two classes of sRNAs: snRNAs and snoRNAs (Figure 2A). By contrast, the NAD cap increase upon HIV-1 infection was detected on sRNAs known to be packed in HIV-1 virions and/or to have increased expression due to HIV-1 infection, particularly Y RNA, and miR19B (Figure 2B).(32-36) Because NAD has not previously been detected on

tRNAs, we did not study them further. Consistent with previous observations,(9) we also detected the NAD cap on 5' end fragments of some mRNAs and, similarly to other cellular RNAs, we observed the reduction of the NAD cap on mRNA upon HIV-1 infection. Nevertheless, we did not study the NAD cap on mRNA further, focusing instead on regulatory RNA. In order to select candidate sRNAs with the greatest increase or depletion of the NAD cap upon HIV-1 infection, we applied a set of criteria to remove sRNA that react nonspecifically in +ADPRC reaction (measured by low enrichment in +ADPRC vs -ADPRC samples), have a low read count, and are inconsistent across replicates (Figure SI3A, Supplemental Excel Table). In particular, we identified four snoRNAs (SNORD3G, SNORD102, SNORA50A, and SNORD3B) and four snRNAs (U1, U4ATAC, U5E, and U7) with loss of the NAD RNA cap upon infection (Figure 2A, B, C, Figure SI3). The highest enrichment (ADPRC-treated samples versus negative control) of NAD-capped RNA was observed for two RNAs, SNORD3B and U1 snRNA (RNU1), in noninfected MT4 cells. The enrichment disappeared after HIV-1 infection, and we observed almost no NAD caps on these two RNAs.

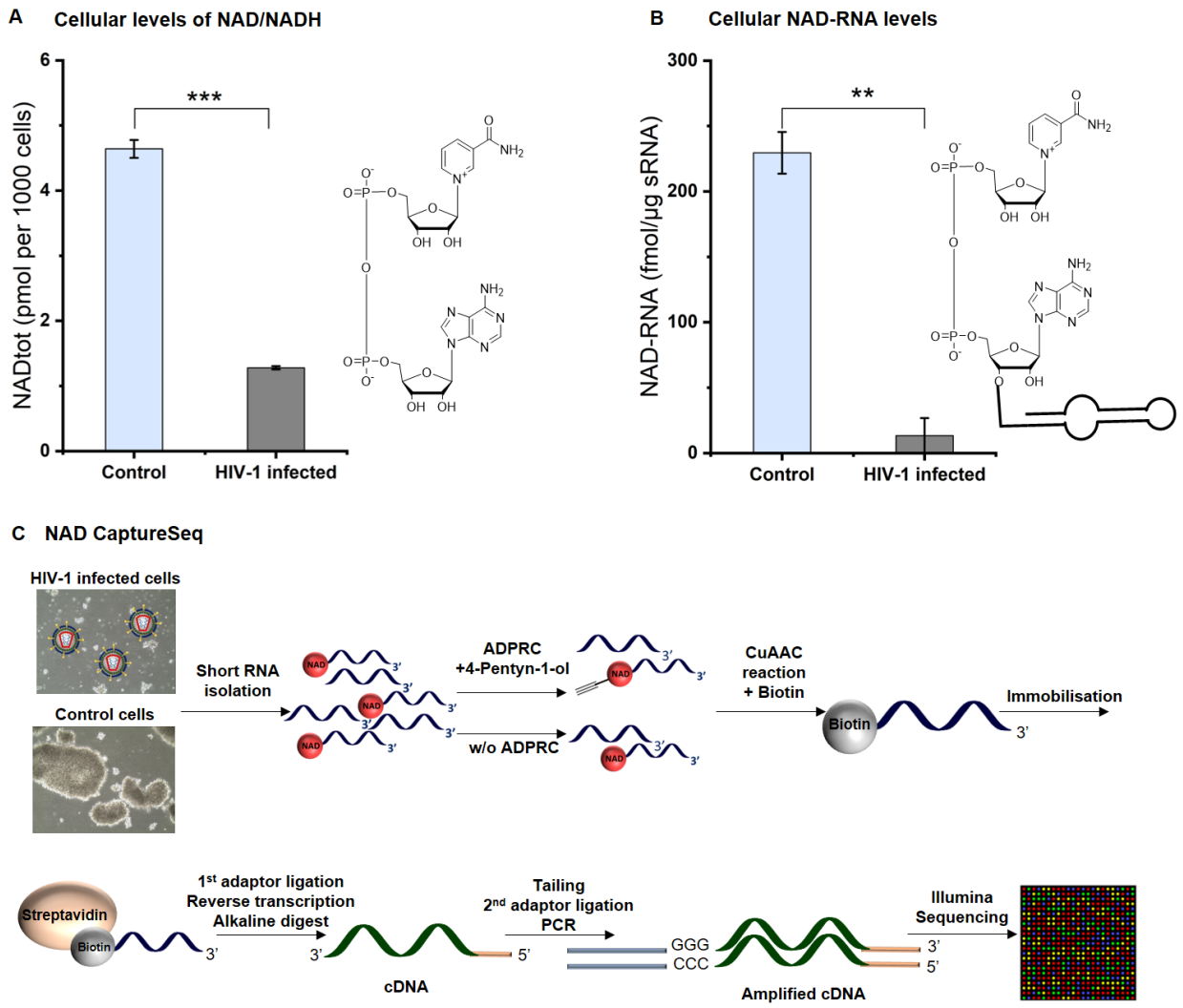

Figure 1: MT-4 cells lose NAD cap upon HIV-1 infection. A) Levels of free NAD/NADH in control and HIV-1 infected cells. B) Levels of NAD-RNA in control and HIV-1 infected cells quantified by LC-MS. C) Scheme of the NAD captureSeq protocol applied to control and HIV-1 infected cells.

To investigate whether the decreased amount of NAD-cap on particular sRNAs after HIV-1 infection is not just a consequence of altered sRNA expression, we prepared sRNA-seq libraries from noninfected and infected cells. Out of 2014 detected sRNAs (miRNAs, miscRNAs, tRNAs, snRNAs, snoRNAs and rRNAs), 89 were identified as significantly differentially expressed - 52 sRNAs were upregulated and 37 downregulated after infection (TableSI2, Figure SI4). Neither of these 89 sRNAs was enriched in NAD captureSeq protocol. Moreover, using this data, we confirmed that the expression levels of identified snRNA and snoRNA do not change after HIV-1 infection (Figure 2D). The enrichment of NAD-RNA in control cells but not in HIV-1 infected cells without the change in RNA expression levels was further validated by RT-PCR of selected sRNAs (Figure SI5). These experiments exclude the possibility that the disappearance of NAD-RNA enrichment in infected cells is caused by the loss of a particular cellular RNA upon HIV-1 infection.

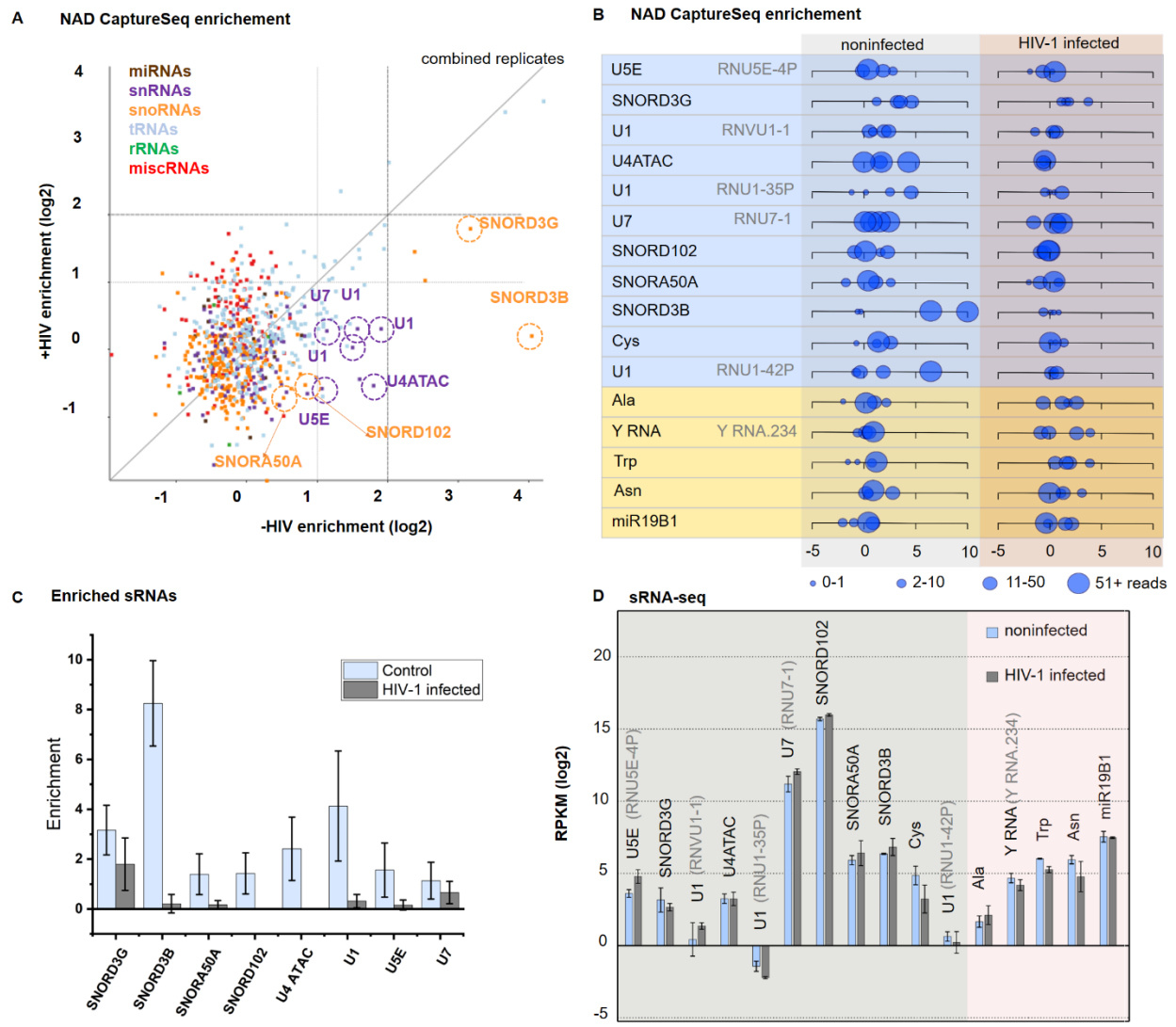

Figure 2: NAD CaptureSeq enrichment of particular sRNAs. A) Scatter plot showing the enrichment (+ADPRC vs -ADPRC) in noninfected and HIV-1 infected samples. B) List of the best candidates with altered NAD capping after HIV-1 infection. The beads show enrichment (+ADPRC vs -ADPRC) noninfected and HIV-1 infected for individual replicates. The size of the bead corresponds to the number of reads in the +ADPRC sample.C) Enrichment of selected RNAs with decreased NAD capping after HIV-1 infection

observed in NAD captureSeq libraries. D) sRNA-seq analysis of expression of identified candidate sRNAs in noninfected and HIV-1 infected cells.

Role of the NAD cap in U1 snRNA in HIV-1 infections

Among the RNAs that lose the NAD cap upon HIV-1 infection, snRNA U1 is known to play an important role in the lifecycle of HIV-1.(22, 37-39) The U1 5' region (8 nucleotides) binds complementary to the 5' splice site of unspliced HIV-1 mRNA (env region), which leads to rev-regulated translocation of partially spliced or unspliced HIV-1 mRNA into cytosol.(21) The single mutation in the 5' splice site of HIV-1 mRNA causes a significant decrease of HIV-1 replication. This effect was suppressed by cotransfection with U1 that restores base pairing with the mutated 5' splice site of HIV-1 mRNA, which indicates the importance of U1 – HIV-1 mRNA base pairing.(21)

Therefore, we investigated the role of the 5' RNA cap of U1 in binding to HIV-1 mRNA. Until now, it was assumed that U1 is naturally capped only by the TMG cap.(23) Here, we show that part of cellular pool of U1 is also capped by NAD and that this cap is depleted upon HIV-1 infection. We recently presented that some noncanonical RNA caps (e.g. Ap_3G) bind to the DNA template via noncanonical base pairing during transcription(40). Accordingly, we hypothesize that the NAD RNA cap may contribute to binding of U1 to its target HIV-1 mRNA and may negatively or positively influence the strength of the interaction. To test this hypothesis, we prepared 20-mer mimicking the 5' U1 RNA region with either the NAD or TMG cap (Supplementary protocol) through in vitro transcription with T7 polymerase (the sequence in positions +2 and +3 was adjusted accordingly) and pseudouridine triphosphate (ΨTP) instead of UTP, and we measured the melting temperature (T_m) values of corresponding duplexes with complementary 20-mer HIV-1 mRNA (Figure 3A). These duplexes were characterized using light cycler (Figure 3B). The T_m of RNA duplexes (under used conditions) were 70.5±0.6 °C and 64.6±0.8°C for TMG-U1 and NAD-U1, respectively. As in vitro transcription with ΨTP did not lead to sufficient amount of RNA for circular dichroism spectroscopy (CD) studies which are usually used for RNA duplex characterization, we prepared 20-mer mimicking the 5' U1 RNA region with either the NAD or TMG cap without ΨTP. The CD spectra of both duplexes with positive maximum at 264 nm were typical for the right-handed A-type double helix of RNA (Figure SI6) and confirmed the observation from light cycler. NAD-U1 pre-mRNA duplex was less stable than TMG-U1 pre-mRNA duplex. This experiment showed that the binding of TMG-U1 to HIV-1 mRNA is much stronger than the NAD-U1 interaction with HIV-1 mRNA. This observation indicates that the NAD cap reduces binding of U1 to the target HIV-1 mRNA sequence and thus may negatively influence HIV-1 replication.

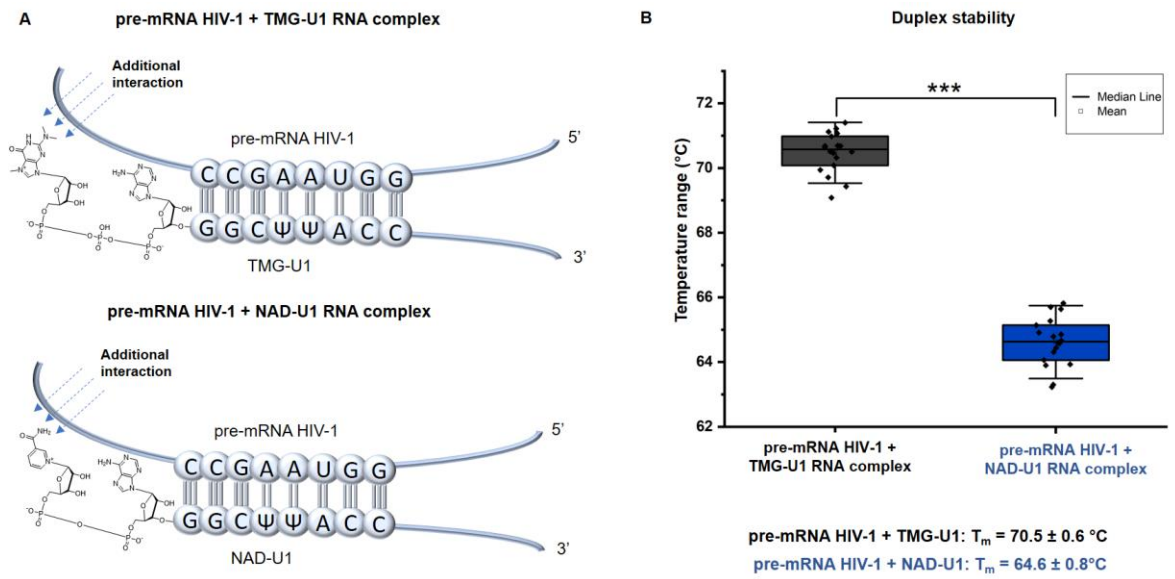

Figure 3: NAD cap of U1 snRNA destabilizes the complex with HIV-1 pre-mRNA. A) Scheme of complex formed by complemental regions of pre-mRNA HIV-1 with either TMG-U1 (left) or NAD-U1 (right). B) Duplex stability measurement of pre-mRNA HIV-1 with TMG-U1 (dark grey) or NAD-U1 (blue) by light cycler.

DXO processing of NAD-RNA in HIV-1 infected cells

The NAD cap is removed in human cells by two enzymes: Nudt12 and DXO. A member of the NudiX family, Nudt12 cleaves the pyrophosphate backbone of free NAD(41) and NAD-RNA and thus reduces the intracellular concentrations of free NAD and NAD-RNA, while DXO cleaves the entire moiety of NAD from RNA and does not affect the intracellular concentration of free NAD (Figure 4A).(9) To investigate solely the role of NAD-RNA (not free NAD) in HIV-1 infection, we focused on the DXO decapping enzyme. Although it has been previously reported that DXO may cleave the TMG cap,(42) we show that NAD-RNA is its preferred substrate (Figure 4B). First, we explored whether the depletion of NAD RNA caps in HIV-1 infected cells is not caused by upregulation of DXO upon infection; however, the western blot analysis showed that levels of DXO are similar in control and HIV-1 infected cells (Figure SI7).

Using lentiviral vectors, we prepared control cells in which we either overexpressed (MT4-DXO OE) or downregulated (MT4-DXO KD) DXO. The efficiency of lentiviral overexpression and knockdown of DXO in MT4 cells was tested by western blot analysis (Figure 4C). Indeed, overexpression of DXO led to a significant increase of the enzyme in the transduced cells, while DXO was almost completely diminished in the knockdown MT4 cells.

Following introduction of lentiviral vectors, we infected transduced MT4-DXO OE and MT4-DXO KD cells with HIV-1. After four days of HIV-1 infection, we evaluated the effect of DXO expression on HIV-1 infectivity by performing HIV-1 titre determination (Figure 4D). The infectivity of HIV-1 in MT4-DXO KD cells was comparable to HIV-1 infectivity in wild-type MT4 cells. In contrast, overexpression of the NAD-RNA decapping enzyme DXO led to a twelvefold increase in the infectivity of HIV-1 in comparison with control cells.

We also followed the effect of DXO overexpression and knockdown on the NAD RNA cap level in a fraction of sRNA (Figure 4E). We quantified the NAD RNA cap level in DXO-overexpressed and DXO-knockdown

MT4 cells (Figure SI1) by LC-MS. The NAD cap level for the RNA isolated from the MT4 DXO knockdown cells was similar to that obtained from the control. This can be explained by the redundancy of decapping enzymes in general.(43, 44) The other decapping enzyme present, Nudt12, may take over the function of the downregulated enzyme DXO. On the other hand, overexpression of the decapping enzyme DXO led to a more than twofold decrease of the NAD cap level in sRNA. This confirms that DXO is responsible for the decapping of NAD from sRNA. Together, these data strongly suggest that the DXO enzyme promotes HIV-1 replication. The result also indicates that the presence of the NAD RNA cap inhibits HIV-1 production and that NAD-RNAs play a role in antiviral defence.

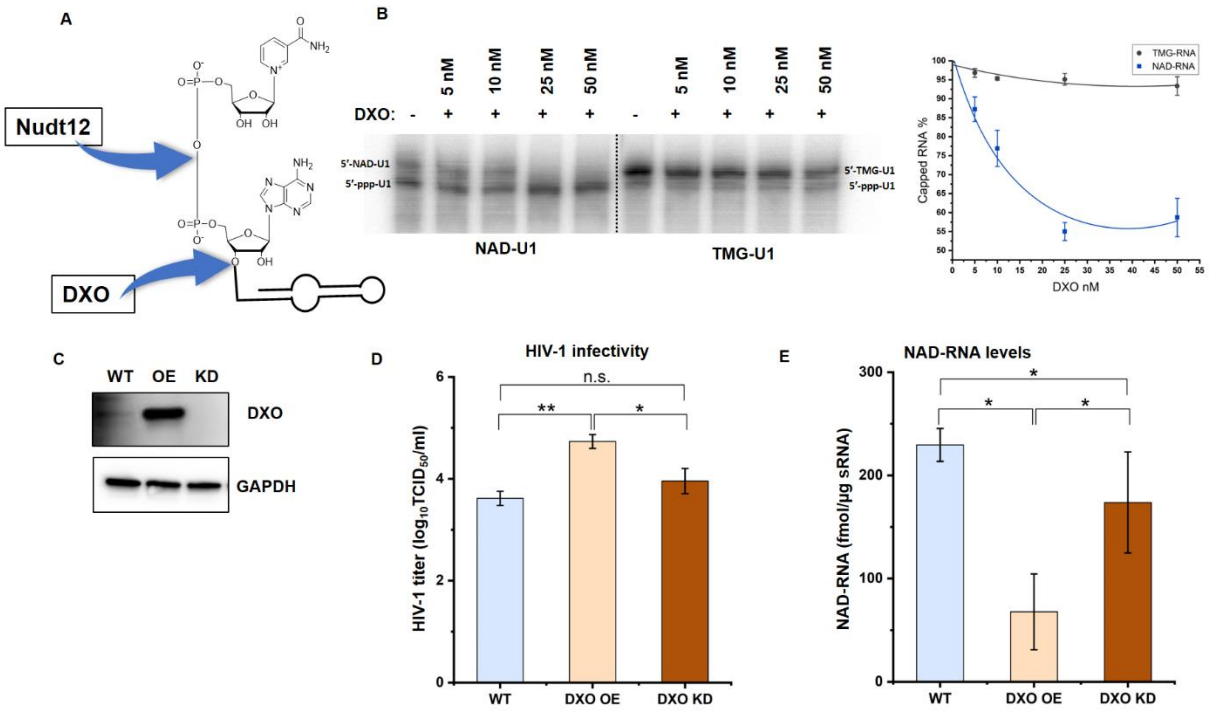

Figure 4: Decrease of NAD RNA capping leads to increase of HIV-1 infectivity. A) Cleavage positions of the NAD RNA cap by two known decapping enzymes: Nudt12 and DXO. B) In vitro DXO cleavage of NAD-U1 and TMG-U1 at various DXO concentrations (5 nM, 10 nM, 25 nM and 50 nM. C) Western blot analysis of DXO and GAPDH (as control) in control cells (WT) and cells with overexpressed (OE) or downregulated (KD) DXO. D) HIV-1 infectivity determinations in control cells (WT) and cells with overexpressed (DXO OE) or downregulated (DXO KD) DXO. E) LC-MS quantification of the NAD RNA cap level in sRNA isolated from control cells (WT) and cells with overexpressed (DXO OE) or downregulated (DXO KD) DXO.

To reveal the effect of NAD repletion on HIV-1 infections, we fed cells with Nicotinamide (NAm, metabolic precursor of NAD) and first, we measured the total cellular concentration of NAD in noninfected cells, HIV-1 infected cells, cells with overexpressed DXO and HIV-1 infected cells with overexpressed DXO with and without addition of NAm (Figure 5A). We observed almost 2-fold change in the intracellular concentration of NAD in noninfected and HIV-1 infected cells after addition of NAm. Less significant (only 1.5-fold) change was observed for NAD concentration in cells with overexpressed DXO and the most prominent was increase of NAD concentration in HIV infected cells with overexpressed DXO after addition of NAm. We also measured how the addition of NAm influences NAD-RNA pool. In all cases, amount of NAD-RNA

significantly increased. The most distinct (almost 3-fold) was increasing of NAD-RNA in HIV-1 infected cells and cells with overexpressed DXO (Figure 5B, Figure SI1).

To study the effect of NAm addition(11, 18) on U1 NAD capping, we selectively captured (45) U1 RNA from sRNA fraction from noninfected cells, HIV-1 infected cells, cells with overexpressed DXO and HIV-1 infected cells with overexpressed DXO with and without addition of NAm (Figure 5C, Figure SI8). This was followed by Nuclease P1 digestion and LC-MS analysis. We calculated the amount of NAD per injected U1 RNA. While in noninfected cells approximately 7 % of U1 bear NAD cap, the amount increases to almost 10 % in cells fed with NAm. HIV-1 infection leads to decrease of U1 NAD capping to less than 5 %. The repletion of NAD restores NAD capping even in infected cells to 7 %. Overexpression of NAD decapping enzyme DXO leads to significant decrease to almost 3 %. Again, addition of NAm increases NAD capping of U1 in cells with overexpressed DXO to 6 %. Due to the sequence similarity, U1 probes are not specific only for U1 sRNA variants identified by our NAD CaptureSeq analysis but also recognise U1 sRNA variants without detected NAD cap. Therefore, the true NAD-capping levels in specific U1 variants can be higher than detected values.

We also study effect of the addition of NAm to HIV-1 infectivity by performing HIV-1 titre determination (Figure 5D). The infectivity of HIV-1 in both types of cells: MT4 and MT4-DXO OE was significantly lower after addition of NAm. This confirms observation from older works and shows that NAD and its precursor have inhibitory effect on HIV-1 infectivity.

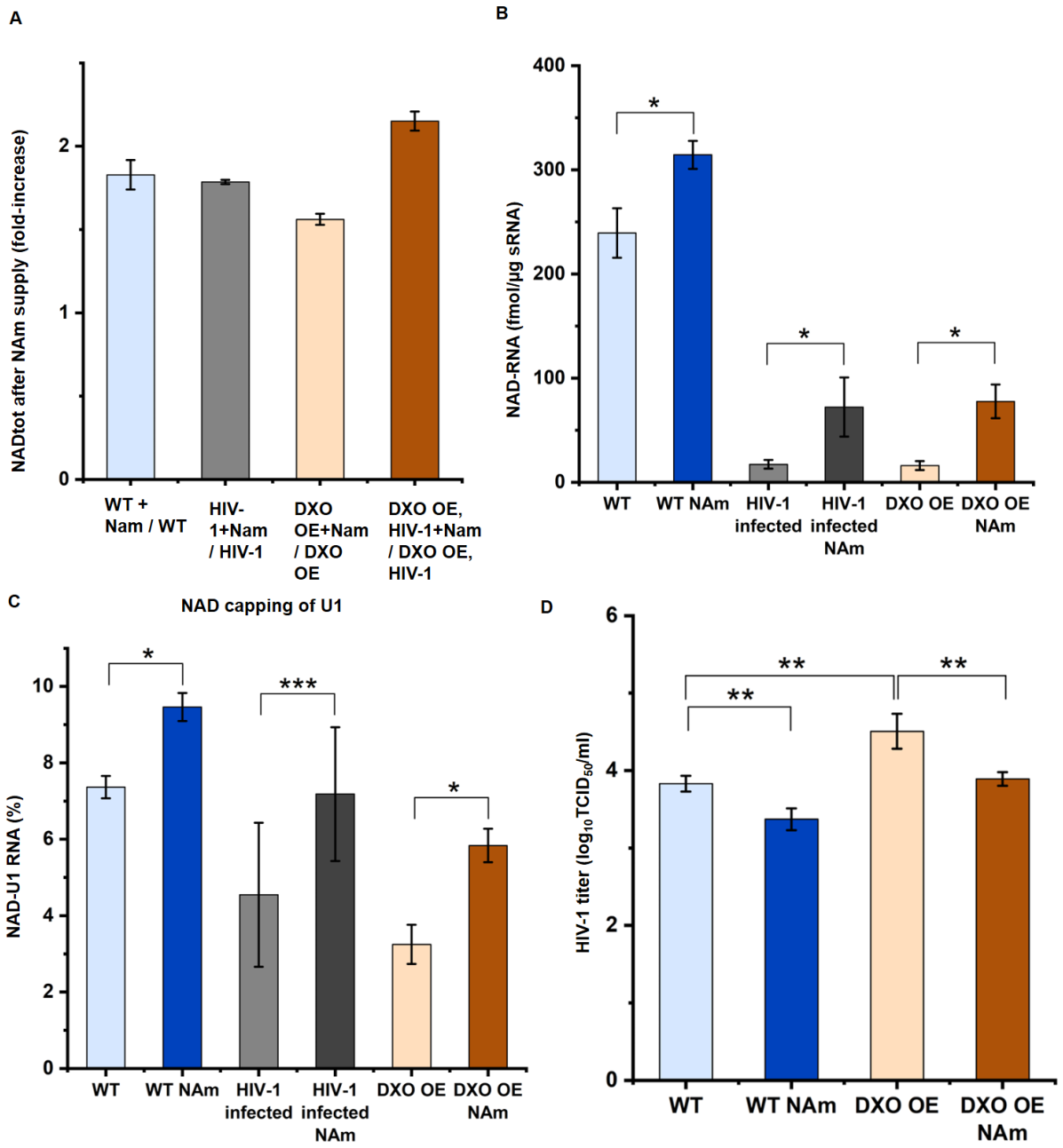

Figure 5: NAm repletion leads to higher NAD capping and lower HIV-1 infectivity. A) Comparison of total NAD/NADH cellular levels (fold-increase) in noninfected cells (WT+NAm/WT), HIV-1 infected cells (HIV-1+NAm/HIV-1), noninfected cells with overexpressed DXO (DXO OE+NAM/DXO OE), and HIV-1 infected cells with overexpressed DXO (DXO OE HIV-1+NAm/DXO OE HIV-1) supplied with NAm and without NAm. B) Comparison of amount of NAD-RNA in noninfected cells (WT), HIV-1 infected cells and cells with overexpressed DXO without and with supplied NAm. C) Quantification and comparison of NAD RNA cap on isolated U1-RNA from noninfected cells, HIV-1 infected cells, and cells with overexpressed DXO without and with supplied NAm. D) HIV-1 infectivity determinations in control cells (WT) and cells with overexpressed (DXO OE) without or with supplied NAm (WT NAm, DXO OE NAm).

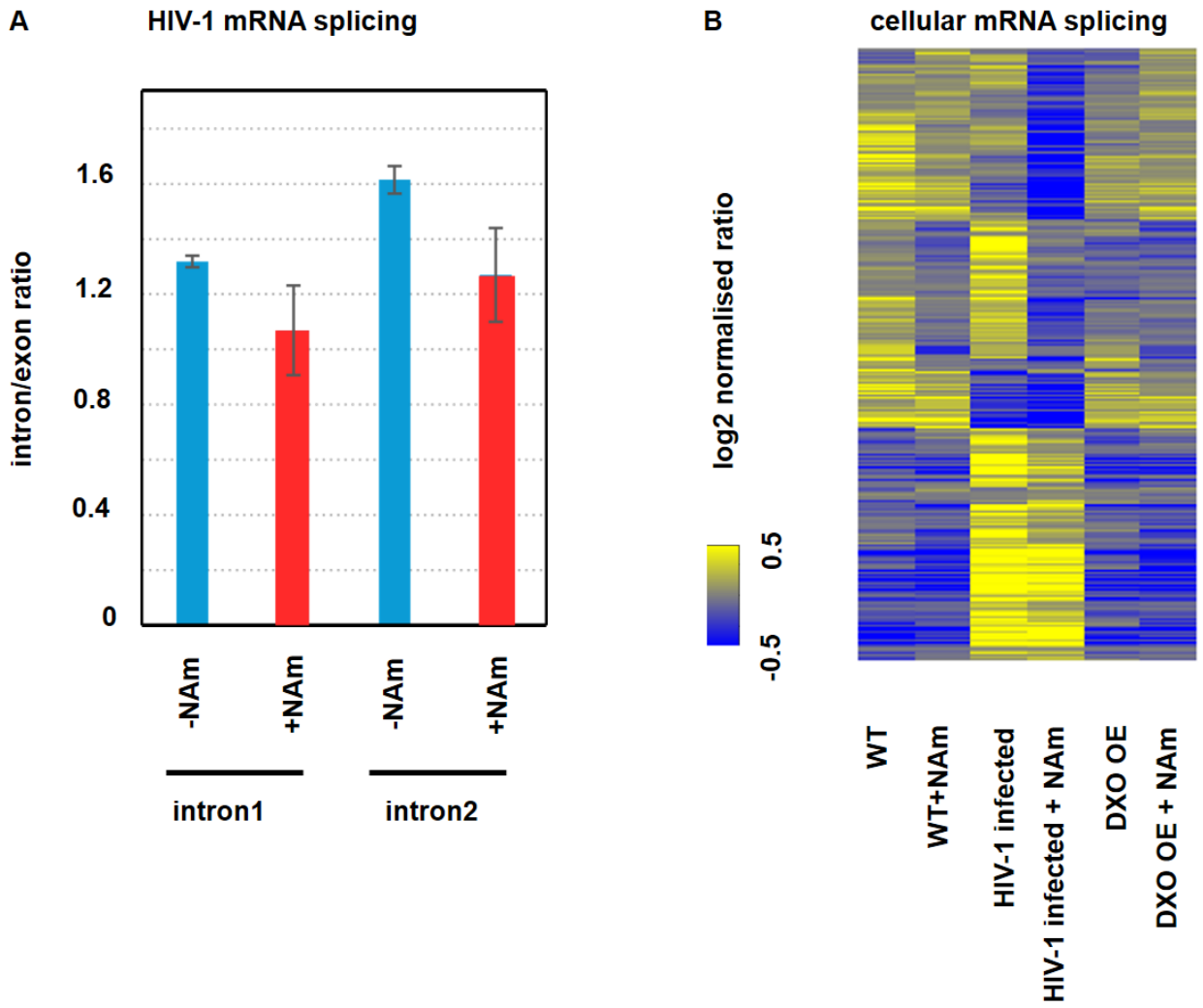

Figure 6: Effect of NAm addition to HIV-1 and cellular splicing. A) HIV-1 mRNA splicing. Intron/exon ratio in two splicing regions (intron 1 and 2) in viral mRNA before and after addition of HIV-1. B) Heat map of cellular mRNA splicing of 1000 most expressed genes. Addition of NAm leads to more efficient splicing in noninfected cells (WT) and HIV-1 infected cells. Splicing in cells with overexpressed DXO is not altered by NAm addition.

As U1 RNA is one of the main components of spliceosome, we explored how NAD capping of U1 influences HIV-1 mRNA and cellular splicing, in general (Figure 6). Therefore, we prepared three replicates of RNA-seq libraries of total ribosomal-depleted RNA from noninfected cells, HIV-1 infected cells and cells with overexpressed DXO before and after addition of NAm. Even though in vitro, the binding of NAD-U1 to HIV-1 pre-mRNA is lower than binding of TMG-U1, we observed that addition of NAm, i.e. increasing of NAD U1 capping, led to more efficient splicing of both HIV-1 mRNA introns (1 and 2) (Figure 6A). This was also the case for the host cellular mRNAs. Here, we show comparison of mRNA splicing for 1000 top expressed genes (Figure 6B). Addition of NAm increased splicing (decreased intron/exon ratio) in noninfected cells as well as in HIV-1 infected cells. The effect was not observed for cells with overexpressed DXO. This finding shows that NAD RNA capping may play a role in cellular splicing and may finally explain functional role of NAD cap in mammalian cells.

Discussion

We applied NAD captureSeq on RNA isolated from control and HIV-1 infected cells. Bioinformatic analysis revealed that subsets of snoRNA (SNORD3G, SNORD102, SNORA50A, and SNORD3B) and snRNA (U1, U4ATAC, U7, and U5E) lose the NAD RNA cap upon HIV-1 infection. Further sRNA-seq and RT-PCR analysis of RNA isolated from HIV-1 infected/control cells and cDNA after NAD captureSeq showed that the level of subsets of snoRNA and snRNA stays unaffected by HIV-1 infection and that the populations of these RNAs differ only in the NAD cap level. As U1 snRNA was reported to be essential for HIV-1 replication, we focused on interaction of this snRNA with HIV-1 pre-mRNA. We prepared a 5' fragment of U1 snRNA containing pseudouridines with either the canonical TMG cap or the NAD cap. We studied the influence of the NAD cap on binding of U1 snRNA to its target sequence in HIV-1 pre-mRNA. Based on our measurement of duplex stability using a light cycler system, we conclude that the presence of the NAD cap significantly destabilizes the binding of U1 snRNA to HIV-1 pre-mRNA by 6°C. CD spectra of these duplexes without naturally present pseudouridines also showed lower stability of NAD-U1 in duplex with HIV-1 pre-mRNA by 2°C in comparison with TMG-U1. The difference in the stability of duplexes with and without pseudouridine may be explained by rigidity caused by pseudouridines, which restricts the motion of neighbouring nucleotides including 5' cap.(46, 47) This indicates that base-pairing of RNA containing the NAD cap with complemental strand is weaker than base-pairing of RNA with the canonical TMG cap. This is the first example of NAD-cap influence on the function of noncoding RNA in mammalian cells.

We also used cells with reduced expression or overexpression of the NAD-decapping enzyme DXO to test whether the NAD cap influences HIV-1 infection. The overexpression of DXO led to a decrease of the NAD RNA cap in general and to a significant increase of HIV-1 infectivity (Figure 7). Opposite effect was observed when the pool of NAD was repleted by addition of NAm. Higher concentration of free NAD and NAD-RNA led to lower infectivity of HIV-1 virus. The supplementation of NAm to HIV-1 infected cells compensated the effect of infection on NAD-U1 capping and lead to increase in NAD capping to levels equal to noninfected cells.

Bioinformatic analysis of splicing patterns in noninfected, HIV-1 infected cells and cells with overexpressed DXO before and after addition of NAm showed that increased NAD capping led to more efficient splicing in HIV-1 encoded mRNA and in cellular mRNAs. This is in agreement with the fact that excessive splicing of HIV-1 mRNA also decreases HIV-1 replication. (22, 48) Finding that the HIV-1 mRNA splicing is more efficient after addition of NAm, i.e when U1 has more NAD cap, is not consistent with our finding that NAD-U1 binds less efficiently to HIV-1 pre-mRNA than TMG-U1. Nevertheless, it is known that duplex formation of HIV-1 pre-mRNA with U1 RNA does not commit this RNA to splicing.(21) Partially spliced or unspliced RNA (HIV-1 pre-mRNA, future genomic RNA) is transported into the cytoplasm, where it is translated into e.g. HIV envelope protein (encoded in partially spliced variant) or serve as genomic RNA in newly formed viral particles. Thus, U1 has dual role in the HIV-1 infection. Besides canonical splicing of HIV-1 mRNA, it helps to transport unspliced variants of HIV-1 pre-mRNA to cytosol and potentially protect them from degradation (Figure 7).

Therefore, we speculate that NAD-capped RNAs restrain HIV-1 replication. Subsequently, decrease of the NAD-capped RNA pool is part of the virus strategy to overcome it. Moreover, our work may provide an explanation for the finding that the polymorphism within the 5' UTR region of the DXO gene in an African American cohort of HIV-1 patients(49) is associated with an altered response to HIV-1 infection. Even though the mutation in the 5' UTR region does not influence the protein sequence itself, it may influence

RNA stability or translatability and thus the intracellular level of DXO protein, which in turn alters the efficiency of HIV-1 replication.

Furthermore, our experiments show direct impact of NAD RNA capping on cellular splicing. This finding has potential to explain much needed functional role of noncanonical RNA caps in eukaryotic cells. For the first time, our work connects noncanonical RNA capping, RNA splicing, innate immunity and antiviral defence.

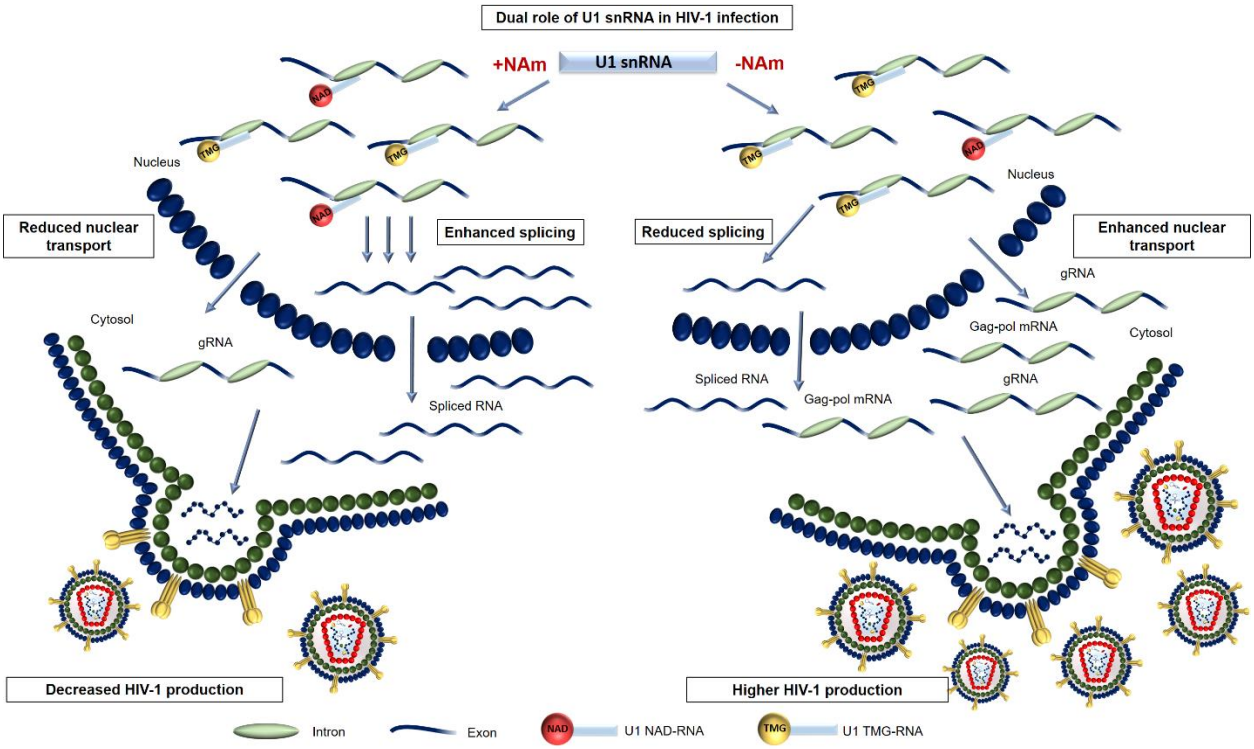

Figure 7: Dual role of U1 sn RNA in HIV-1 infection. Left: Higher concentration of cellular NAD (after addition of NAm) leads to higher NAD capping of U1 and more efficient splicing of HIV-1 mRNA, but lower transport of HIV-1 pre-mRNA into cytosol. This results in decreased HIV-1 replication. Right: Natural depletion of cellular NAD by HIV-1 infection leads to decreased NAD capping of U1 and less efficient splicing of HIV-1 mRNA, but more efficient transport of HIV-1 pre-mRNA from nucleus to cytosol. HIV-1 virus has available all portfolio of spliced, alternatively spliced or unspliced RNA essential for its replication and thus the virus production is more efficient.

Acknowledgements

We are grateful to all members of the Cahova Group for their help and advice, particularly Zuzana Buchova and Maria-Bianca Mititelu for DXO preparation. We acknowledge funding from the Ministry of Education, Youth and Sports (Czech Republic), programme ERC CZ (LL1603) and European Research Council Executive Agency (ERCEA) under the European Union's Horizon Europe Framework Programme for Research and Innovation (grant agreement No 101041374 - StressRNaction). D. S. acknowledges the Czech Science Foundation (#21-04132S). Computational resources were supplied by the project "e-Infrastruktura CZ" (e-INFRA CZ LM2018140) supported by the Ministry of Education, Youth and Sports (Czech Republic). Data are accessible in the GEO database under accession GSE191019.

Author Contributions

B.B. and H.C. designed experiments and coordinated the project. B.B., R.B., J.T., K.G., L.B. and H.C. performed experiments. K.G. and J. K. prepared TMG and coordinated chemical synthesis. J.P., J.W., D.S. designed experiments. L.B. measured CD spectra. Z.K. designed and coordinated preparation of OE and KD DXO. L.G. performed all bioinformatic analysis. H.C. supervised the work. B.B. and H.C. wrote the paper.

References

1. P. Boccaletto *et al.*, MODOMICS: a database of RNA modification pathways. 2017 update. *Nucleic Acids Research* **46**, D303-D307 (2017).
2. W. E. Kowtoniuk, Y. Shen, J. M. Heemstra, I. Agarwal, D. R. Liu, A chemical screen for biological small molecule–RNA conjugates reveals CoA-linked RNA. *Proceedings of the National Academy of Sciences* **106**, 7768-7773 (2009).
3. Y. G. Chen, W. E. Kowtoniuk, I. Agarwal, Y. Shen, D. R. Liu, LC/MS analysis of cellular RNA reveals NAD-linked RNA. *Nature Chemical Biology* **5**, 879 (2009).
4. O. Hudeček *et al.*, Dinucleoside polyphosphates act as 5'-RNA caps in bacteria. *Nature Communications* **11**, 1052 (2020).
5. H. Cahová, M.-L. Winz, K. Höfer, G. Nübel, A. Jäschke, NAD captureSeq indicates NAD as a bacterial cap for a subset of regulatory RNAs. *Nature* **519**, 374 (2014).
6. M.-L. Winz *et al.*, Capture and sequencing of NAD-capped RNA sequences with NAD captureSeq. *Nature Protocols* **12**, 122 (2016).
7. H. G. Morales-Filloy *et al.*, The 5'-NAD cap of RNAIII modulates toxin production in Staphylococcus aureus isolates. *Journal of Bacteriology* 10.1128/jb.00591-19, JB.00591-00519 (2019).
8. R. W. Walters *et al.*, Identification of NAD+ capped mRNAs in Saccharomyces cerevisiae. *Proc. Natl. Acad. Sci. U. S. A.* **114**, 480-485 (2017).
9. X. Jiao *et al.*, 5' End Nicotinamide Adenine Dinucleotide Cap in Human Cells Promotes RNA Decay through DXO-Mediated deNADding. *Cell* **168**, 1015-1027.e1010 (2017).
10. Y. Wang *et al.*, NAD⁺-capped RNAs are widespread in the Arabidopsis transcriptome and can probably be translated. *Proceedings of the National Academy of Sciences* **116**, 12094-12102 (2019).
11. M. F. Murray, M. Nghiem, A. Srinivasan, HIV infection decreases intracellular nicotinamide adenine dinucleotide [NAD]. *Biochem Biophys Res Commun* **212**, 126-131 (1995).
12. A. Savarino *et al.*, Investigation of the potential role of membrane CD38 in protection against cell death induced by HIV-1. *J Biol Regul Homeost Agents* **10**, 13-18 (1996).
13. J. C. Rodríguez-Alba *et al.*, HIV Disease Progression: Overexpression of the Ectoenzyme CD38 as a Contributory Factor? *Bioessays* **41**, e1800128 (2019).
14. A. Savarino, F. Bottarel, F. Malavasi, U. Dianzani, Role of CD38 in HIV-1 infection: an epiphenomenon of T-cell activation or an active player in virus/host interactions? *Aids* **14**, 1079-1089 (2000).
15. E. W. Taylor, The oxidative stress-induced niacin sink (OSINS) model for HIV pathogenesis. *Toxicology* **278**, 124-130 (2010).

16. G. Furlini, M. C. Re, M. La Placa, Increased poly(ADP-ribose)polymerase activity in cells infected by human immunodeficiency virus type-1. *Microbiologica* **14**, 141-148 (1991).
17. F. Fallarino *et al.*, T cell apoptosis by tryptophan catabolism. *Cell Death Differ* **9**, 1069-1077 (2002).
18. M. F. Murray, A. Srinivasan, Nicotinamide inhibits HIV-1 in both acute and chronic in vitro infection. *Biochem Biophys Res Commun* **210**, 954-959 (1995).
19. M. F. Murray, Niacin as a potential AIDS preventive factor. *Med Hypotheses* **53**, 375-379 (1999).
20. M. F. Murray, Nicotinamide: an oral antimicrobial agent with activity against both Mycobacterium tuberculosis and human immunodeficiency virus. *Clin Infect Dis* **36**, 453-460 (2003).
21. X. B. Lu, J. Heimer, D. Rekosh, M. L. Hammarskjöld, U1 small nuclear RNA plays a direct role in the formation of a rev-regulated human immunodeficiency virus env mRNA that remains unspliced. *Proc Natl Acad Sci U S A* **87**, 7598-7602 (1990).
22. D. Mandal, Z. Feng, C. M. Stoltzfus, Excessive RNA splicing and inhibition of HIV-1 replication induced by modified U1 small nuclear RNAs. *J Virol* **84**, 12790-12800 (2010).
23. J. Hamm, E. Darzynkiewicz, S. M. Tahara, I. W. Mattaj, The trimethylguanosine cap structure of U1 snRNA is a component of a bipartite nuclear targeting signal. *Cell* **62**, 569-577 (1990).
24. K. E. Ocwieja *et al.*, Dynamic regulation of HIV-1 mRNA populations analyzed by single-molecule enrichment and long-read sequencing. *Nucleic Acids Research* **40**, 10345-10355 (2012).
25. H. Sertznig, F. Hillebrand, S. Erkelenz, H. Schaal, M. Widera, Behind the scenes of HIV-1 replication: Alternative splicing as the dependency factor on the quiet. *Virology* **516**, 176-188 (2018).
26. A. Mlynarska-Cieslak *et al.*, Nicotinamide-Containing Di- and Trinucleotides as Chemical Tools for Studies of NAD-Capped RNAs. *Organic Letters* **20**, 7650-7655 (2018).
27. F. Huang, Efficient incorporation of CoA, NAD and FAD into RNA by in vitro transcription. *Nucleic Acids Research* **31**, e8-e8 (2003).
28. G. Nübel, F. A. Sorgenfrei, A. Jäschke, Boronate affinity electrophoresis for the purification and analysis of cofactor-modified RNAs. *Methods* **117**, 14-20 (2017).
29. T. Kafri, U. Blömer, D. A. Peterson, F. H. Gage, I. M. Verma, Sustained expression of genes delivered directly into liver and muscle by lentiviral vectors. *Nature Genetics* **17**, 314-317 (1997).
30. J. G. Bird *et al.*, The mechanism of RNA 5’ capping with NAD+, NADH and desphospho-CoA. *Nature* **535**, 444 (2016).
31. Y. Zhang *et al.*, Extensive 5’-surveillance guards against non-canonical NAD-caps of nuclear mRNAs in yeast. *Nature Communications* **11**, 5508 (2020).
32. M. J. Eckwahl *et al.*, Analysis of the human immunodeficiency virus-1 RNA packageome. *RNA* 10.1261/rna.057299.116 (2016).
33. A. Telesnitsky, S. Wolin, The Host RNAs in Retroviral Particles. *Viruses* **8**, 235 (2016).
34. A. Šimonová *et al.*, LC/MS analysis and deep sequencing reveal the accurate RNA composition in the HIV-1 virion. *Scientific Reports* **9**, 8697 (2019).
35. L.-B. Yin *et al.*, Elevated Expression of miR-19b Enhances CD8+ T Cell Function by Targeting PTEN in HIV Infected Long Term Non-progressors With Sustained Viral Suppression. *Frontiers in Immunology* **9** (2019).
36. K. Duskova *et al.*, MicroRNA regulation and its effects on cellular transcriptome in human immunodeficiency virus-1 (HIV-1) infected individuals with distinct viral load and CD4 cell counts. *BMC Infect Dis* **13**, 250 (2013).
37. R. Sajic *et al.*, Use of modified U1 snRNAs to inhibit HIV-1 replication. *Nucleic Acids Res* **35**, 247-255 (2007).

38. M. P. Ashe, A. Furger, N. J. Proudfoot, Stem-loop 1 of the U1 snRNP plays a critical role in the suppression of HIV-1 polyadenylation. *Rna* **6**, 170-177 (2000).
39. M. P. Ashe, L. H. Pearson, N. J. Proudfoot, The HIV-1 5' LTR poly(A) site is inactivated by U1 snRNP interaction with the downstream major splice donor site. *Embo j* **16**, 5752-5763 (1997).
40. R. Benoni, M. Culka, O. Hudeček, L. Gahurova, H. Cahová, Dinucleoside Polyphosphates as RNA Building Blocks with Pairing Ability in Transcription Initiation. *ACS Chemical Biology* **15**, 1765-1772 (2020).
41. S. R. Abdelraheim, D. G. Spiller, A. G. McLennan, Mammalian NADH diphosphatases of the Nudix family: cloning and characterization of the human peroxisomal NUDT12 protein. *Biochem J* **374**, 329-335 (2003).
42. X. Jiao, J. H. Chang, T. Kilic, L. Tong, M. Kiledjian, A mammalian pre-mRNA 5' end capping quality control mechanism and an unexpected link of capping to pre-mRNA processing. *Mol Cell* **50**, 104-115 (2013).
43. J. Carreras-Puigvert *et al.*, A comprehensive structural, biochemical and biological profiling of the human NUDIX hydrolase family. *Nat Commun* **8**, 1541 (2017).
44. Y. Li, M. Song, M. Kiledjian, Differential utilization of decapping enzymes in mammalian mRNA decay pathways. *Rna* **17**, 419-428 (2011).
45. C. E. Dumelin, Y. Chen, A. M. Leconte, Y. G. Chen, D. R. Liu, Discovery and biological characterization of geranylated RNA in bacteria. *Nature Chemical Biology* **8**, 913-919 (2012).
46. P. Auffinger, E. Westhof, "Effects of Pseudouridylation on tRNA Hydration and Dynamics: a Theoretical Approach" in Modification and Editing of RNA. (1998), https://doi.org/10.1128/9781555818296.ch6, pp. 103-112.
47. M. I. Newby, N. L. Greenbaum, A conserved pseudouridine modification in eukaryotic U2 snRNA induces a change in branch-site architecture. *Rna* **7**, 833-845 (2001).
48. A. Emery, R. Swanstrom, HIV-1: To Splice or Not to Splice, That Is the Question. *Viruses* **13**, 181 (2021).
49. K. Pelak *et al.*, Host determinants of HIV-1 control in African Americans. *J Infect Dis* **201**, 1141-1149 (2010).